

# Development of Split-Window Algorithm for Land Surface Temperature Estimation From the VIRR/FY-3A Measurements

Geng-Ming Jiang, *Member, IEEE*, Wei Zhou, and Ronggao Liu

**Abstract**—This letter addressed the development of split-window algorithm to estimate land surface temperature (LST) from the measurements acquired by the Visible and Infrared Radiometer on FengYun 3A using radiative transfer modeling experiment with the moderate spectral resolution atmospheric transmittance algorithm and computer model and the SeaBor V5.0 database. To improve the accuracy, the total precipitable water and the mean of land surface emissivities (LSEs) and LST were divided into several subranges. The split-window algorithm was applied to the Northeastern China area ( $115^{\circ}$  E– $135^{\circ}$  E,  $40^{\circ}$  N– $55^{\circ}$  N), and then, the estimated LSTs were cross-validated with the Terra Moderate Resolution Imaging Spectroradiometer (MODIS/Terra) LST and Emissivity (LST/E) V5 products: MOD11C1 V5 and MOD11\_L2 V5. The results show that the LSTs in this work are averagely consistent with the MODIS/Terra LST/E V5 products with accuracy better than 1.0 K: The errors are  $0.5 \pm 0.9$  K and  $0.0 \pm 0.9$  K for daytime and nighttime, respectively, when the retrieved LSTs were compared to the MOD11C1 V5 product, while the errors are  $0.6 \pm 0.9$  K and  $0.0 \pm 0.9$  K for daytime and nighttime, respectively, when the results were compared to the MOD11\_L2 V5 product.

**Index Terms**—Algorithms, brightness temperature, estimation, infrared sensors, land surface temperature, low earth orbit satellites.

## I. INTRODUCTION

LAND surface temperature (LST) is a key parameter in the physics of land surface processes on regional as well as a global scale, combining the results of all surface–atmosphere interactions and energy fluxes between the atmosphere and the ground [1]. The major challenges in LST estimation from satellite thermal infrared data are the removals of the effects caused by atmospheric attenuation, land surface emissivity (LSE), and topography [2]. The LST estimation methods include the single-channel method [3], [4], the split-window method [5], [6], and the multichannel method, e.g., the day/night method [7] and the temperature/emissivity separation method [8]. Because

Manuscript received January 20, 2013; revised February 26, 2013 and March 25, 2013; accepted March 26, 2013. Date of publication April 12, 2013; date of current version May 27, 2013. This work was supported by the National Natural Science Foundation of China under Grants 41271012 and 40901158.

G.-M. Jiang and W. Zhou are with Key Laboratory of Wave Scattering and Remote Sensing Information, Fudan University, Shanghai 200433, China (e-mail: jianggengming@hotmail.com).

R. Liu is with the Institute of Geographic Sciences and Natural Resources Research, Chinese Academy of Sciences, Beijing 100101, China (e-mail: liurg@reis.ac.cn).

Color versions of one or more of the figures in this paper are available online at <http://ieeexplore.ieee.org>.

Digital Object Identifier 10.1109/LGRS.2013.2255859

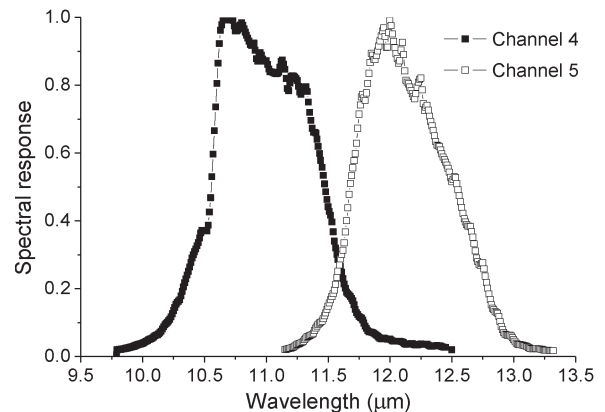


Fig. 1. Spectral response functions of VIRR/FY-3A channels 4 and 5.

of its simplicity and autonomous correction of atmospheric effects, the split-window method is widely used. So far, the split-window method has been successfully applied to the LST retrievals from the data acquired by the Advanced Very High Resolution Radiometer [2], [9], the Moderate Resolution Imaging Spectroradiometer (MODIS) [5], the Spinning Enhanced Visible and Infrared Imager [6], the Stretched Visible and Infrared Spin Scan Radiometer on FengYun 2C satellite [10], and etc.

Two of its second generation polar-orbiting meteorological satellites under the FengYun 3 (FY-3) series were sequentially launched on May 27, 2008, and Nov. 5, 2010, by the China Meteorological Administration, which are referred to as FengYun 3A (FY-3A) and FengYun 3B, respectively. The FY-3A spacecraft carries 11 instruments providing measurements from ultraviolet, visible, infrared to microwave, one of which is the Visible and Infrared Radiometer (VIRR). The VIRR/FY-3 instrument has 10 channels covering from visible to infrared spectrum with nominal spatial resolution of 1.1 km at nadir [11], [12]. VIRR/FY-3A channels 4 ( $10.8 \mu\text{m}$ ) and 5 ( $12.0 \mu\text{m}$ ) are two split-window channels as shown in Fig. 1, and the measurements are suitable for LST retrieval. A split-window method to estimate LST from VIRR/FY-3A measurements had been developed [13]. However, the method is partly problematic, such as the use of 80% of relative humidity as clear-sky criterion and no overlap between two neighboring groups of water vapor contents. Moreover, the results were cross-validated with the 1-km MODIS/Terra LST and Emissivity (LST/E) product MOD11\_L2 only at five locations (including two water bodies) and in four days.

This letter also focused on the development of a split-window algorithm to estimate LST from VIRR/FY-3A measurements, and improvements were made not only in the algorithm development but also in LST retrieval and validation. Including this part, this letter is organized into four sections. Section II describes the development of the split-window algorithm, Section III presents the application of the split-window algorithm to a Northeastern China area, and Section IV is the summary and conclusion.

## II. DEVELOPMENT OF THE SPLIT-WINDOW ALGORITHM

The split-window algorithm presented in [5] was adopted in this work, and it is

$$T_s = C + \left( A_1 + A_2 \frac{1 - \varepsilon}{\varepsilon} + A_3 \frac{\Delta \varepsilon}{\varepsilon^2} \right) \frac{T_i + T_j}{2} + \left( B_1 + B_2 \frac{1 - \varepsilon}{\varepsilon} + B_3 \frac{\Delta \varepsilon}{\varepsilon^2} \right) \frac{T_i - T_j}{2} \quad (1)$$

with  $\varepsilon = (\varepsilon_i + \varepsilon_j)/2$  and  $\Delta \varepsilon = \varepsilon_i - \varepsilon_j$ , where  $T_s$  is the LST and  $T_i$  and  $T_j$  are the brightness temperatures at top-of-atmosphere (TOA) in the channels  $i$  ( $\sim 11.0 \mu\text{m}$ ) and  $j$  ( $\sim 12.0 \mu\text{m}$ ), respectively.  $\varepsilon$  is the mean of the LSEs in the channels  $i$  ( $\varepsilon_i$ ) and  $j$  ( $\varepsilon_j$ ),  $\Delta \varepsilon$  is the LSE difference, and  $C$ ,  $A_1$ ,  $A_2$ ,  $A_3$ ,  $B_1$ ,  $B_2$ , and  $B_3$  are unknown coefficients.

In this letter, the channels  $i$  and  $j$  in (1) correspond to VIRR/FY-3A channels 4 and 5, respectively. The seven unknown coefficients can be obtained through regression with coincident measurements of  $T_4$ ,  $T_5$ ,  $T_s$ , and LSEs in VIRR/FY-3A channels 4 and 5. However, there are no such field measurements available so far. A good solution is to use the radiative transfer modeling experiment, which is conducted by the moderate spectral resolution atmospheric transmittance algorithm and computer model (MODTRAN) [14] fed with currently available atmospheric database, the possible values of land surface variables, and view zenith angles (VZAs).

The SeeBor V5.0 training database of global profiles (<http://cimss.ssec.wisc.edu/>), called the SeeBor V5.0 database for short as follows) was selected in this work. The SeeBor V5.0 database consists of 15 704 global profiles with temperature, moisture, and ozone at 101 pressure levels for clear-sky conditions [15]. Over land, there are a total of 8429 profiles, and the atmospheric temperature at the boundary level ( $T_0$ ) changes from 200.2 K to 318.5 K, while the total precipitable water (TPW) varies from 0.0 to 7.8 cm (only 17 profiles with TPW greater than 6.5 cm). According to the aforementioned description, the SeeBor V5.0 database is very suitable for the numerical experiment.

In the radiative transfer modeling experiment, seven at-surface VZAs were considered:  $0.0^\circ$ ,  $27.5^\circ$ ,  $40.0^\circ$ ,  $47.5^\circ$ ,  $53.75^\circ$ ,  $60.0^\circ$ , and  $65.0^\circ$ . They were selected as a compromise between the Gaussian angles, which characterize the angular variation of the atmospheric quantities [16]. The LST goes from  $T_0 - 5$  to  $T_0 + 20$  K with a step of 5 K. The mean of LSE ( $\varepsilon$ ) changes from 0.90 to 1.0 with a step of 0.02, and the LSE difference ( $\Delta \varepsilon$ ) varies from  $-0.025$  to  $0.015$  with a step of 0.005. The development of the split-window algorithm

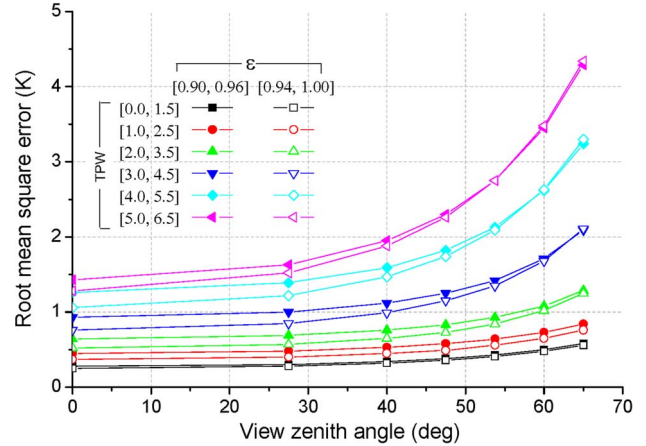


Fig. 2. Regression rmses at the seven VZAs for the subranges of TPW and mean of LSEs, taking LST as a whole.

was accomplished in three steps. First, the total atmospheric transmittance, the total atmospheric upwelling radiance, and the total atmospheric downwelling radiance at the seven VZAs were calculated using MODTRAN for the land profiles extracted from the SeeBor V5.0 database. Then, the brightness temperatures at TOA in VIRR/FY-3A channels 4 and 5 were computed using the radiative transfer equation fed with possible combinations of the atmospheric parameters, LSTs and LSEs. Finally, the seven unknown coefficients in (1) were obtained using the multiple linear regressions [17].

To improve the regression accuracy, the TPW and mean of the LSEs were divided into several tractable subranges. The TPWs were grouped into six subranges with an overlap of 0.5 cm:  $[0, 1.5]$ ,  $[1.0, 2.5]$ ,  $[2.0, 3.5]$ ,  $[3.0, 4.5]$ ,  $[4.0, 5.5]$ , and  $[5.0, 6.5]$  cm, and the mean values of LSEs were divided into two groups with an overlap of values 0.02:  $[0.90, 0.96]$  and  $[0.94, 1.00]$ . Fig. 2 shows the regression root-mean-square errors (rmses) at the seven VZAs for the subranges of TPW and the mean of LSEs. The maximum rmse is up to 4.5 K. To further improve the regression accuracy, the LSTs were divided into four subranges with an overlap of 5 K:  $\leq 282.5$ ,  $[277.5, 297.5]$ ,  $[292.5, 312.5]$ , and  $\geq 307.5$  K. Fig. 3 displays the regression rmses at the seven VZAs for all the subranges of LST, TPW, and the mean of LSEs. The rmse increases with the growth of VZA, TPW, and LST. Compared to the results in Fig. 2, the rmses in Fig. 3 are relatively lower. When the TPW is less than 2.5 cm, the rmses are less than 1.0 K, while, when the TPW is less than 3.5 cm or the VZA is less than  $27.5^\circ$ , the rmses are less than 1.5 K. For example, Fig. 4 shows the coefficients of the developed split-window algorithm for LST from 292.5 K to 312.5 K and TPW from 2.0 to 3.5 cm.

After the development of the split-window algorithm, the LST is estimated in two steps. First, the approximate LST is estimated using the coefficients of the subrange of TPW and the mean of LSEs, taking LST as a whole. Then, accurate LST is derived with the coefficients of the subrange of LST, TPW, and the mean of LSEs. For an arbitrary angle not equal to the seven VZAs, the coefficients were calculated from the coefficients of two neighboring VZAs using the bilinear interpolation method.

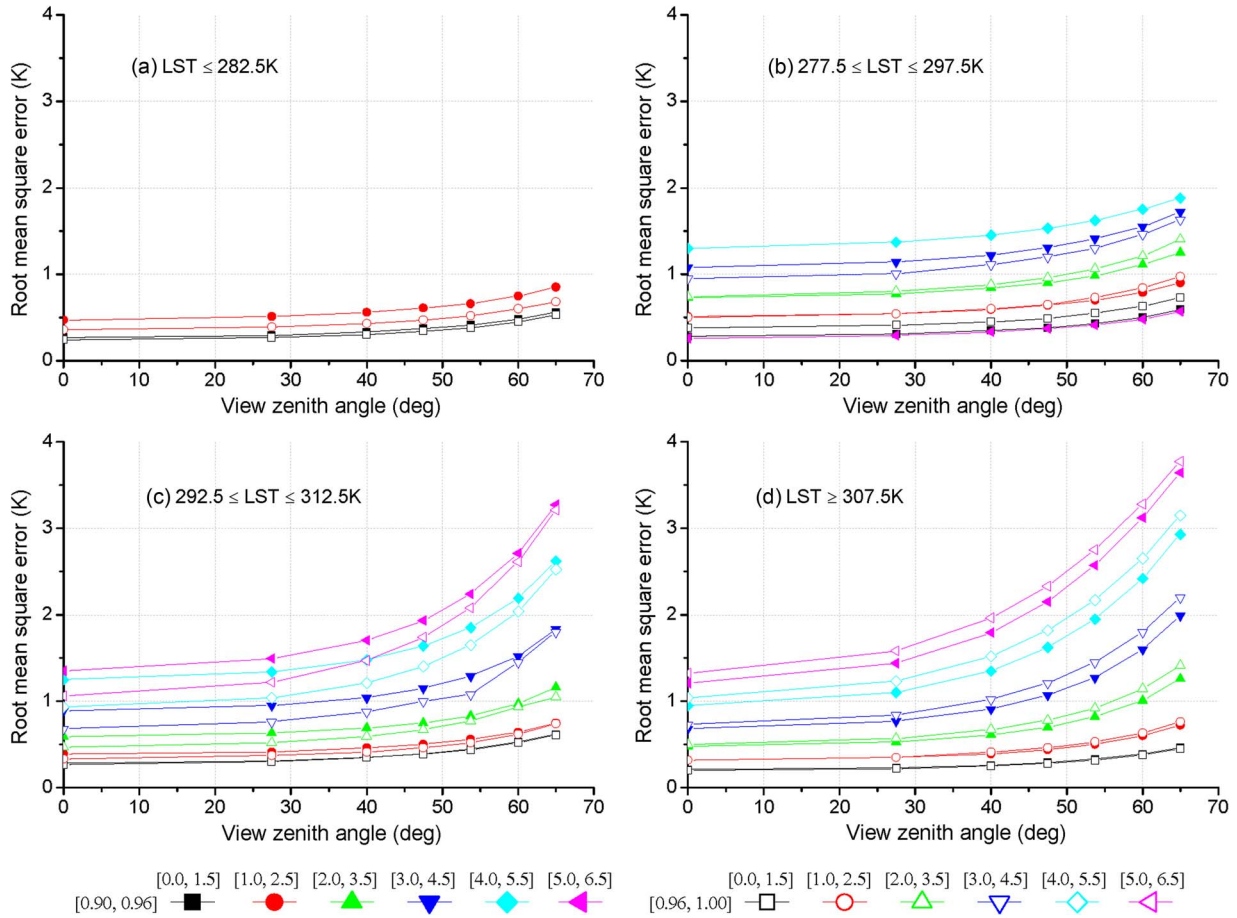


Fig. 3. Regression rmses at the seven VZAs for all the subranges of LST, TPW, and the mean of LSEs.

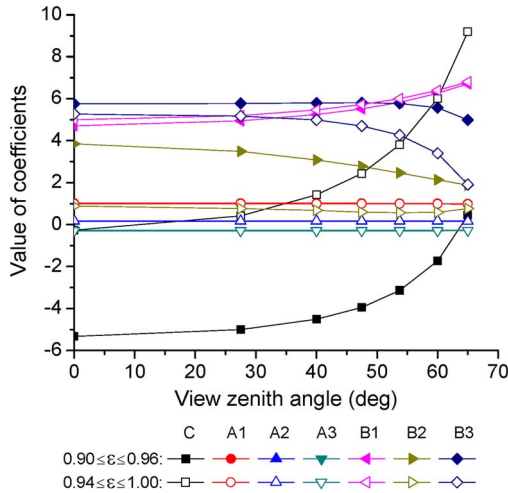


Fig. 4. Coefficients of the developed split-window algorithm for LST from 292.5 K to 312.5 K and TPW from 2.0 to 3.5 cm.

### III. APPLICATION TO THE NORTHEASTERN CHINA AREA

The developed split-window algorithm was applied to LST retrieval from VIRR/FY-3A measurements acquired in September 2010 over a Northeastern China area (115° E–135° E, 40° N–55° N) as shown in Fig. 5. According to the Global Land Cover 2000 (<http://bioval.jrc.ec.europa.eu/products/glc2000/products.php>), this study area mainly consists

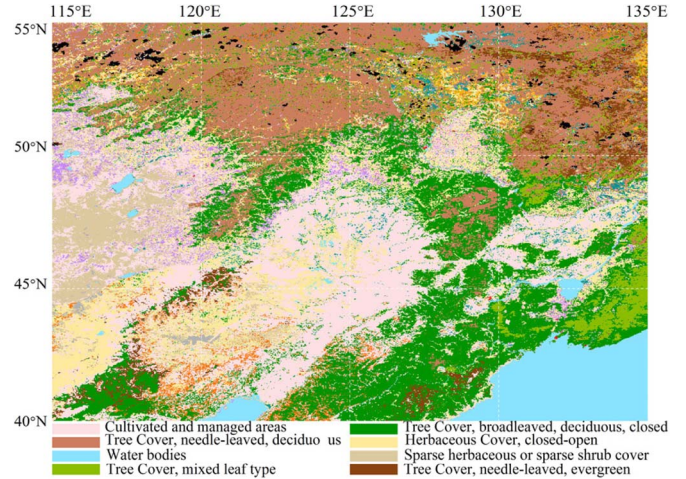


Fig. 5. Study area (generated from Global Land Cover 2000).

of cultivated and managed areas, broadleaved and deciduous tree cover, needle-leaved deciduous tree cover, herbaceous cover, and water bodies. Because of more probability of clear sky, the study time span from September 1 to September 30 of 2010 was selected.

As presented in Section II, the split-window algorithm needs brightness temperatures at TOA, LSEs, VZA, and TPW as input. The brightness temperatures in VIRR/FY-3A channels 4 and 5 and the corresponding VZAs were extracted from the

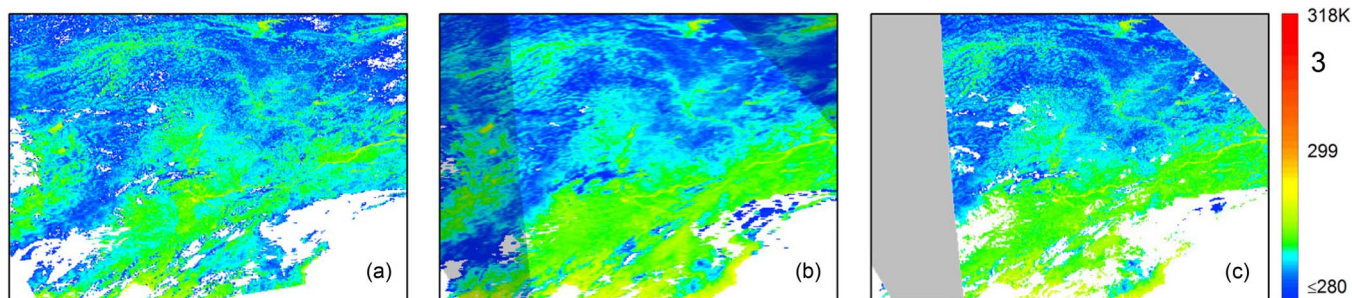


Fig. 6. Maps of (a) LSTs estimated from nighttime VIRR/FY-3A measurements (13:10 September 2, 2010) and the temporally closest LSTs extracted from the (b) MOD11C1 V5 product and (c) MOD11\_L2 V5 product (the gray-masked regions are the overlapping areas of two neighboring orbits of MODIS/Terra).

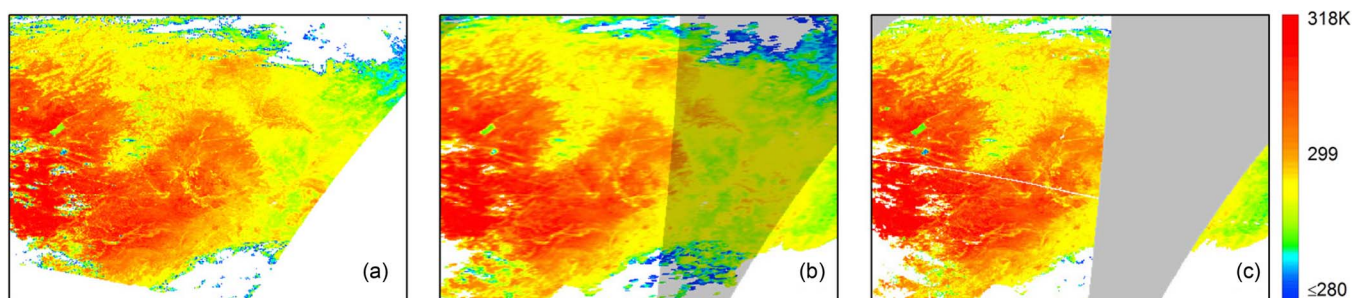


Fig. 7. Maps of (a) LSTs estimated from daytime VIRR/FY-3A measurements (3:10 September 8, 2010) and the temporally closest LSTs extracted from the (b) MOD11C1 V5 product and (c) MOD11\_L2 V5 product (the gray-masked regions are the overlapping areas of two neighboring orbits of MODIS/Terra).

VIRR/FY-3A 1B data product downloaded from the FengYun Satellite Data Center (<http://fy3.satellite.cma.gov.cn>) and then were geometrically transferred into the study area with longitude and latitude resolutions of  $0.05^\circ \times 0.05^\circ$ . Recalibration of the brightness temperatures in VIRR/FY-3A channels 4 and 5 was done according to the results in [18]. The LSEs in VIRR/FY-3A channels 4 and 5 were calculated using the baseline fit method [19] with the LSEs extracted from the MODIS/Terra LST/E V5 product (MOD11C1 V5). The TPWs were extracted from the operational archive European Center for Medium-Range Weather Forecasts (ECMWF) reanalysis data with longitude and latitude resolutions of  $0.125^\circ \times 0.125^\circ$  and then were transferred into the study area using the bilinear interpolation method. As we know, the ECMWF reanalysis data are only available at four Coordinated Universal Time (UTC) times, 0:00, 6:00, 12:00, and 18:00, which are not coincident with VIRR/FY-3A measurements. In this letter, the TPWs temporally closest to VIRR/FY-3A measurements were used in the LST estimation.

The LSTs over the study area in September of 2010 were derived from VIRR/FY-3A measurements using the split-window method developed in this work. As examples, Figs. 6(a) and 7(a) show the maps of LSTs estimated from nighttime and daytime VIRR/FY-3A measurements, respectively. The LSTs vary from 275.0 K to 318.0 K, and daytime LSTs are usually higher than that at night. In the day, the LSTs over the sparsely vegetated areas are generally higher than that over the densely vegetated areas due to the relatively low thermal inertia of soils. However, similar phenomenon is also observed for the nighttime LSTs as shown in Fig. 6(a), because the measurements were acquired shortly after sunset.

The results in this work were cross-validated with the MODIS/Terra LST/E V5 products, i.e., MOD11C1 V5 and

MOD11\_L2 V5, which have been well validated [20]. The MOD11C1 V5 product at  $0.05^\circ$  latitude/longitude climate model grids were generated by reprojection and average of the values in the daily MODIS/Terra LST/E product (MOD11B1) produced by the day/night method [7]. The MOD11\_L2 V5 product is a 5-min level-2 swath 1-km data set and covers both daytime and nighttime acquisitions. In MOD11\_L2 V5 product, the LSEs were estimated by the classification-based emissivity method [21], while the LSTs were derived using the generalized split-window algorithm [5]. The data extracted from the MODIS/Terra LST/E V5 products are LSTs, VZAs, and time of LST observations. The data extracted from the MOD11\_L2 V5 product were geometrically transferred into the study area using the inverse distance weighting interpolation method.

It should be noted that the MOD11C1 V5 product is grid-based global product. Over the overlapping areas of two neighboring orbits of MODIS/Terra, the LSTs are composite. Moreover, the time of LST observations was divided into 12-min stripes. The use of composited LSTs and inaccurate time of LST observations will introduce errors in the cross-validation. In this letter, the cross-validation was carried out only over the areas without overlap, and the accurate time of LST observations was restored from the swath-based MOD11\_L2 V5 product. As examples, the LSTs extracted from the MODIS/Terra LST/E products are also shown in Figs. 6 and 7, and the gray-masked regions are the overlapping areas.

In this letter, the following criteria were used to find out the collocated LST pairs for cross-validation: the absolute time differences of less than 10 min ( $|\Delta T| < 10'$ ) and the absolute VZA differences of less than  $5^\circ$  ( $|\Delta VZA| < 5^\circ$ ). To mitigate the influence of inhomogeneity of land surface properties, the maximum LST difference in a  $3 \times 3$  window centered at the

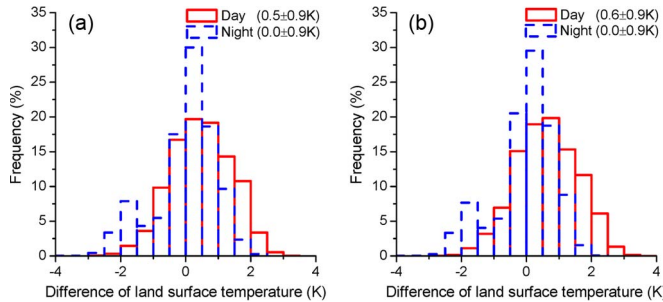


Fig. 8. Histograms of the differences (a) between the LSTs in this work and that extracted from the MOD11C1 V5 product and (b) between the LSTs in this work and that extracted from the MOD11\_L2 V5 product.

matching pixel within an image is required to be less than 2.0 K, i.e., the cross-validation was carried out in relatively homogeneous regions of LSTs. A total of 8087 and 5508 LST matching pairs were picked out for daytime and nighttime, respectively. Fig. 8 displays the histograms of the LST differences between the LSTs in this work and that extracted from the MODIS/Terra LST/E V5 products. The LST differences are basically normally distributed in the range from  $-4.0$  K to  $4.0$  K. The errors are  $0.5 \pm 0.9$  K and  $0.0 \pm 0.9$  K for daytime and nighttime, respectively, when the retrieved LSTs were compared to the MOD11C1 V5 product, while the errors are  $0.6 \pm 0.9$  K and  $0.0 \pm 0.9$  K for daytime and nighttime, respectively, when the results were compared to the MOD11\_L2 V5 product. The results also reveal that the LSTs extracted from the MOD11C1 V5 and MOD11\_L2 V5 products are consistent. Generally, the retrieved LSTs in this work are averagely consistent with the MODIS/Terra LST/E V5 products with accuracy better than 1.0 K.

#### IV. SUMMARY AND CONCLUSION

In this letter, the generalized split-window algorithm to estimate LSTs from VIRR/FY-3A measurements has been developed using radiative transfer modeling experiment with MODTRAN and the SeaBor V5.0 database. To improve the accuracy of the split-window algorithm, VZA, TPW, mean of LSEs, and LST were divided into several subranges.

The developed split-window algorithm was applied to the LST retrieval from VIRR/FY-3A measurements in September of 2010 over the Northeastern China area, and then, the results were cross-validated with the MODIS/Terra LST/E V5 products. The results show that the LSTs in this work are averagely consistent with the MODIS/Terra LST/E V5 products with accuracy better than 1.0 K: The errors are  $0.5 \pm 0.9$  K and  $0.0 \pm 0.9$  K for daytime and nighttime, respectively, when the retrieved LSTs were compared to the MOD11C1 V5 product, while the errors are  $0.6 \pm 0.9$  K and  $0.0 \pm 0.9$  K for daytime and nighttime, respectively, when the results were compared to the MOD11\_L2 V5 product.

The split-window algorithm developed in this letter will be further examined and validated over more areas in the world and in more seasons.

Digital values of the linear regression coefficients in (1) to estimate LSTs from VIRR/FY-3A measurements can be requested via e-mail from jianggengming@hotmail.com.

#### ACKNOWLEDGMENT

The authors would like to thank the anonymous reviewers for their valuable suggestions that improve the quality of this letter.

#### REFERENCES

- [1] P. J. Sellers, F. G. Hall, G. Asrar, D. E. Strebel, and R. E. Murphy, "The first ISLSCP filed experiment (FIFE)," *Bull. Amer. Meteorol. Soc.*, vol. 69, no. 1, pp. 22–27, Jan. 1988.
- [2] J. C. Price, "Land surface temperature measurements from the split window channels of the NOAA 7 advanced very high resolution radiometer," *J. Geophys. Res.*, vol. 89, no. D5, pp. 7231–7237, Aug. 1984.
- [3] Z. Qin, A. Karnieli, and P. Berliner, "A mono-window algorithm for retrieving land surface temperature from Landsat TM data and its application to the Israel–Egypt border region," *Int. J. Remote Sens.*, vol. 22, no. 18, pp. 3719–3746, 2001.
- [4] J. C. Jiménez-Muñoz and J. A. Sobrino, "A generalized single-channel method for retrieving land surface temperature from remote sensing data," *J. Geophys. Res.*, vol. 108, no. D22, pp. 4688–4696, Nov. 2003.
- [5] Z. Wan and J. Dozier, "A generalized split-window algorithm for retrieving land-surface temperature from space," *IEEE Trans. Geosci. Remote Sens.*, vol. 34, no. 4, pp. 892–905, Jul. 1996.
- [6] G.-M. Jiang and Z.-L. Li, "Split-window algorithm for land surface temperature estimation from MSG1-SEVIRI data," *Int. J. Remote Sens.*, vol. 29, no. 20, pp. 6067–6074, Oct. 2008.
- [7] Z. Wan and Z.-L. Li, "A physics-based algorithm for retrieving land-surface emissivity and temperature from EOS/MODIS data," *IEEE Trans. Geosci. Remote Sens.*, vol. 35, no. 4, pp. 980–996, Jul. 1997.
- [8] A. R. Gillespie, S. Rokugawa, T. Matsunaga, J. S. Cothren, S. Hook, and A. B. Kahle, "A temperature and emissivity separation algorithm for Advanced Spaceborne Thermal Emission and Reflection Radiometer (ASTER) images," *IEEE Trans. Geosci. Remote Sens.*, vol. 36, no. 4, pp. 1113–1126, Jul. 1998.
- [9] Y. H. Kerr, J. P. Lagouarde, and J. Imbernon, "Accurate land surface temperature retrieval from AVHRR data with use of an improved split-window algorithm," *Remote Sens. Environ.*, vol. 41, no. 2/3, pp. 197–209, Aug./Sep. 1992.
- [10] B.-H. Tang, Y. Y. Bi, Z.-L. Li, and J. Xia, "Generalized split-window algorithm for estimate of land surface temperature from Chinese geostationary FengYun meteorological satellite (FY-2C) data," *Sensors*, vol. 8, no. 2, pp. 933–951, Feb. 2008.
- [11] C. Dong, J. Yang, W. Zhang, Z. Yang, N. Lu, J. Shi, P. Zhang, Y. Liu, and B. Cai, "An overview of a new Chinese weather satellite FY-3A," *Bull. Amer. Meteorol. Soc.*, vol. 90, no. 10, pp. 1531–1544, Oct. 2009.
- [12] Z. Yang, N. Lu, J. Shi, P. Zhang, C. Dong, and J. Yang, "Overview of FY-3 payload and ground application system," *IEEE Trans. Geosci. Remote Sens.*, vol. 50, no. 12, pp. 4846–4853, Dec. 2012.
- [13] J. Jiang, Q. Liu, H. Li, and H. Huang, "Split-window method for land surface temperature estimation from FY-3A/VIRR data," in *Proc. IEEE IGARSS*, Jul. 2011, pp. 305–308.
- [14] A. Berk, L. S. Bernstein, G. P. Anderson, P. K. Acharya, D. C. Robertson, J. H. Chetwynd, and S. M. Adler-Golden, "MODTRAN cloud and multiple scattering upgrades with application to AVIRIS," *Remote Sens. Environ.*, vol. 65, no. 3, pp. 367–375, Sep. 1998.
- [15] E. E. Borbas, S. W. Seemann, H.-L. Huang, J. Li, and W. P. Menzel, "Global profile training database for satellite regression retrievals with estimates of skin temperature and emissivity," in *Proc. 14th Int. ATOVS Study Conf.*, May 2005, pp. 763–770.
- [16] Z. Wan and J. Dozier, "Land surface temperature measurements from space: Physical principles and inverse modeling," *IEEE Trans. Geosci. Remote Sens.*, vol. 27, no. 3, pp. 268–278, May 1989.
- [17] D. F. Andrews, "A robust method for multiple linear regression," *Technometrics*, vol. 16, no. 4, pp. 523–531, Nov. 1974.
- [18] G.-M. Jiang and S.-H. Liu, "Intercalibration of infrared window channels of FY-3A instruments against AIRS/Aqua data," in *Proc. Int. Conf. Multimedia Technol.*, Oct. 2010, pp. 1–4.
- [19] S. W. Seemann, E. E. Borbas, R. Q. Knuteson, G. R. Stephenson, and H.-L. Huang, "Development of a global infrared land surface emissivity database for application to clear sky sounding retrievals from multi-spectral satellite radiance measurements," *J. Appl. Meteorol. Climatol.*, vol. 47, no. 1, pp. 108–123, Jan. 2008.
- [20] Z. Wan, "New refinements and validation of the MODIS land-surface temperature/emissivity products," *Remote Sens. Environ.*, vol. 112, no. 1, pp. 59–74, Jan. 2008.
- [21] W. C. Snyder, Z. Wan, Y. Zhang, and Y.-Z. Feng, "Classification-based emissivity for land surface temperature measurement from space," *Int. J. Remote Sens.*, vol. 19, no. 14, pp. 2753–2774, Sep. 1998.